Hindawi Publishing Corporation
Journal of Chemistry
Volume 2015, Article ID 349830, 7 pages
http://dx.doi.org/10.1155/2015/349830

Research Article

Actual Application of a H_2-Based Polyvinyl Chloride Hollow Fiber Membrane Biofilm Reactor to Remove Nitrate from Groundwater

Yanhao Zhang,[1,2] Lilong Huang,[1] Zhibin Zhang,[1] Cuizhen Sun,[1] and Jixiang Li[3]

[1]*School of Municipal and Environmental Engineering, Shandong Jianzhu University, Jinan 250101, China*
[2]*State Key Laboratory of Pollution Control and Resource Reuse, Tongji University, Shanghai 200092, China*
[3]*Sustainable Technology Research Center, Shanghai Advanced Research Institute, Chinese Academy of Sciences, Shanghai 201210, China*

Correspondence should be addressed to Zhibin Zhang; zhazhb@163.com

Received 24 April 2014; Accepted 27 October 2014

Academic Editor: Tian C. Zhang

To evaluate the actual performance of the H_2-based polyvinyl chloride hollow fiber membrane biofilm reactor (HF-MBfR), we used HF-MBfR to remove nitrate from the nitrate contaminated groundwater with the dissolved oxygen (~6.2 mg/L) in Zhangqiu city (Jinan, China). The reactor was operated over 135 days with the actual nitrate contaminated groundwater. The result showed that maximum of nitrate denitrification rate achieved was over 133.8 g NO_3^--N/m^3d (1.18 g NO_3^--N/m^2d) and the total nitrogen removal was more than 95.0% at the conditions of influent nitrate 50 mg/L, hydrogen pressure 0.05 MPa, and dissolved oxygen (DO) 6.2 mg/L, with the nitrate in effluent under the value limits of drinking water. The fluxes analysis showed that the electron-equivalent fluxes of nitrate, sulfate, and oxygen account for about 81.2%, 15.2%, and 3.6%, respectively, which indicated that nitrate reduction could consume more electrons than that of sulfate reduction and dissolved oxygen reduction. The nitrate reduction was not significantly influenced by sulfate reduction and the dissolved oxygen reduction. Based on the actual groundwater quality on site, the Langelier Saturation Index (LSI) was 0.4, and the membrane could be at the risk of surface scaling.

1. Introduction

Currently, nitrate contamination of drinking water supplies has become a serious problem in the world. If the level of nitrate in water exceeds 10 mg N/l (WHO), methemoglobinemia in infants or blue baby syndrome would occur, and nitrosamines, that is, potential carcinogenic metabolites of nitrate, would be formed [1–3].

The best available technologies (BAT) for NO_3^- removal from drinking water include ion exchange [4], reverse osmosis [5], and electrodialysis [6, 7]. However, the utilities of these processes were limited due to their expensive operation and subsequent disposal problem of the generated nitrate waste brine [8]. Biological denitrification is carried out by facultative bacteria that can use NO_3^- as a terminal electron acceptor for respiration under anoxic conditions. The microorganisms that participated in the processes (i.e., heterotrophic denitrification and autotrophic denitrification) are genetically diverse and metabolically versatile [9]. Basically, organic substrates such as methanol or ethanol were used in the process of heterotrophic denitrification because organic carbon concentrations in drinking water are very low [10]. Therefore, the cost increases and the second pollutions also could appear.

Autotrophic denitrification using hydrogen as the supplemental donor has been extensively investigated to remove nitrate from polluted drinking water or waste water [11–14]. The autohydrogenotrophic denitrifiers are able to respire on NO_3^--N in the absence of molecular oxygen. Otherwise, hydrogen is cheaper and nontoxic and of lower biomass yield and without a residual [15, 16]. The following equations could describe the stoichiometry of hydrogenotrophic denitrification [15]:

$$NO_3^- + H_2 \longrightarrow NO_2^- + H_2O \quad (1)$$

$$NO_2^- + 0.5H_2 + H^+ \longrightarrow NO + H_2O \quad (2)$$

$$2NO + H_2 \longrightarrow N_2O + H_2O \quad (3)$$

$$N_2O + H_2 \longrightarrow N_2 + H_2O \quad (4)$$

$$2NO_3^- + 2H^+ + 5H_2 \longrightarrow N_2 + 6H_2O \quad (5)$$

Using hydrogen to reduce nitrate or other oxidants in water had been studied through sparging gas or bubbleless gas [11, 13, 17]. Due to the danger of explosion and low hydrogen utilization for the sparging methods, bubbleless gas-permeable membrane technology has developed to a promising way to reduce nitrate. Bubbleless gas-permeable membranes had been studied before including different composite membrane, including nonporous polyurethane layers [17], polypropylene [18], silicone-coated reinforced fiberglass fibers [16], and silicone-coated ferronickel slag [19]. The nitrate reducing processes normally could achieve a good effect of denitrification in the absence of oxygen, because of the oxygen always being a competitor for the electron acceptors. Therefore, most of the hydrogenotrophic denitrification processes were operated in the absence of oxygen in laboratories, while, for the nitrate contaminated drinking water, including surface water or shallow groundwater, dissolved oxygen (DO) is often present in the contaminated waters and is the favored electron accepter for hydrogen oxidizing bacteria. On the other hand, membrane fouling is not clear in the MBfR, although there are lots of studies about membrane fouling on membrane bioreactor (MBR), while, in MBR it is the contaminated water with SS that goes through the micropores of the membrane in order to get purified water or to hold back the particles. However, in MBfR it is the pressured hydrogen that goes through the membrane pores to provide the hydrogen for utilization by the hydrogenotrophic bacteria on the membrane surface. Therefore, the fouling mechanisms are different for MBR and MBfR. Otherwise, there are still some problems that limited the application for the MBfR, such as the inconvenient hydrogen supply and lower hydrogen utilization rate.

The objective of this study was to investigate the actual performance of polyvinyl chloride (PVC) membrane biofilm reactor for removing nitrate from groundwater, especially to assess the influences of DO and membrane fouling on the process.

2. Materials and Methods

2.1. Membrane Biofilm Reactor. The HF-MBfR used in this study is shown in Figure 1. A transparent plastic cylinder was used as a hollow fiber membrane reactor, in which two membrane modules were directly submerged in the bulk fluid and gas sealed with the plastic ring and the cap of the reactor (Figure 1). The reactor was 22 cm in height and 6 cm in inner diameter. The system made the feed-media mix well in the biofilm reactor because the stirring power was generated by a magnetic stirrer set in the bottom of the reactor. The hollow fibers were made of PVC with pore size of 0.01 μm, manufactured by Litree Company (Suzhou, China). The outside and inner diameters of the fiber are 0.15 and 0.085 cm, respectively, which provides 633.3 cm^2 of surface area with total 96 hollow fibers (each module consisted of 48 hollow fibers). The total available volume of the reactor system was 560 mL. The void ratio of the working reactor volume (volume of fiber was 23.7 mL) was 95.8%. A single peristaltic pump (Longer BT50-1J, Baoding, China) was used to keep a nitrate-medium-feed rate of 1.1 mL/min. Pure H_2 was supplied to the inside hollow fibers through a H_2 gas tank via a metering value.

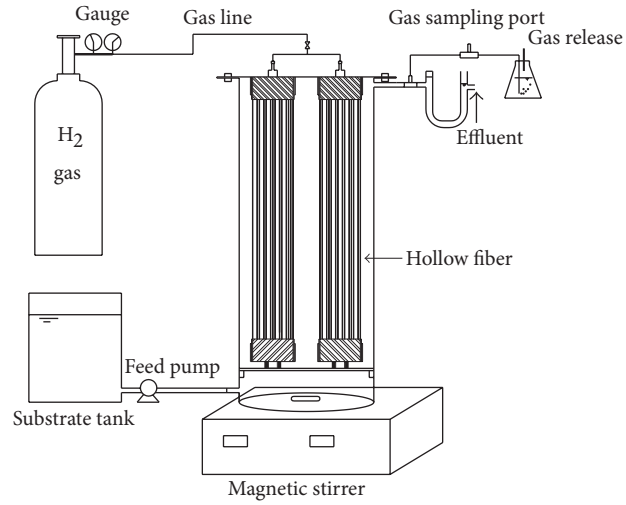

Figure 1: Schematic of the MBfR.

2.2. Influent of Nitrate Contaminated Shallow Groundwater. In the present study, the feeding medium was taken from the groundwater in the vegetable land at the suburb of Zhangqiu city (Jinan, China), where a lot of fertilizers had been used in the lands. Therefore, the shallow groundwater around the vegetable land had been contaminated by nitrate, and the water quality was shown in Table 1.

2.3. Start-Up and Experimental Conditions. Start-up of the continuous stirred MBfR began when hydrogen was supplied to the membrane under the hydrogen pressure of 0.03 MPa, and the MBfR had been acclimated for several months in our laboratory. The flow rate was 1.1 mL/min with the HRT 8.5 h, and the MBfR was operated over 135 days. To reduce the influent shock loading for the biofilm, the pumped groundwater had been diluted by tap water. The detailed operation conditions of the reactor were listed in Table 2.

2.4. Analytical Method. All the fluid samples collected from the reactor were kept in the refrigerator at 4°C and analyzed within 2 days. The concentrations of NO_3^--N, NO_2^--N, and SO_4^{2-}, hardness, alkalinity, TDS, and pH value were analyzed according to Chinese NEPA standard methods [20]. DO was measured by a DO probe (Hach, HQ40d). The gas sample in the headspace of the reactor was taken by inserting a gas-tight syringe through the rubber stopper on the gas-sampling port. The gas concentrations were measured by a GC 14-B quipped with a TCD detector (Shimadazu Co.). The liquid

Table 1: Water quality for the groundwater.

Total dissolved solids (mg/L)	pH	DO (mg/L)	Alkalinity (mg/L as $CaCO_3$)	Hardness (mg/L as $CaCO_3$)	Nitrate (mg N/L)	Nitrite (mg N/L)	Sulfate (mg/L)
300–400	7.5~7.8	5.5~6.5	400~600	150~250	45~55	ND	80~90

Table 2: Operation conditions of the membrane biofilm reactor.

	Run I	Run II	Run III
Operation period (day)	1–36	37–81	82–135
H_2 pressure (MPa)	0.03	0.04	0.05
Influent NO_3^--N (mg/L)	20.0 ± 2.0	40.0 ± 4.0	50.0 ± 4.0
Hydraulic retention time (h)		8.5	

phase concentrations of H_2 in the reactor were calculated by H_2 headspace concentrations using Henry's law.

For the SEM experiment, a part of a new control PVC membrane fiber was obtained by a sterile shaver and cleaned with distilled water and then dried and coated with Au/Pb in order to enhance the quality of the images. After the preparation, the fiber was examined by scanning electron microscope (SEM, XL-30, Philips, Netherlands). The samples of fiber at running stages were checked by SEM using the same methods without the preparation of washing [21, 22].

3. Results and Discussion

3.1. Denitrification Performance of Continuous Stirred MBfR. Under the condition of HRT 8.5 h, the influent concentrations of nitrate ranged from 20 to 50 mg N/L (Table 1), and the influent concentrations of sulfate ranged from 40 to 90 mg SO_4^{2-}/L through the experiments with the hydrogen pressure varied from 0.03 to 0.05 MPa. In Run I of the first 36 days, the biofilm was successfully switched to the new influent from the synthetic influent and the concentrations of nitrate and sulfate in the effluent dropped gradually to 0.3 mg N/L and 24.0 mg SO_4^{2-}/L, respectively, and the nitrite was not detected in the final phase of the periods (Figure 2). Although the DO in the influent was maintained at about 6.2 ± 0.3 mg/L, the TN removal also reached about 98.3 ± 2.5%, and the effluent DO was about 0.2 mg/L, which indicated that the electron acceptor nitrate and oxygen could get hydrogen electron donor easier than sulfate.

At Run II and Run III, the hydrogen pressures were adjusted to 0.04 and 0.05 MPa, respectively, and the influent nitrate was adjusted to 40 and 50 mg N/L. The results showed that the average removal efficiencies of nitrate in Runs I and II were 98.8% and 95.1%, respectively. In the effluent, the average of residual nitrate concentrations was about 0.5 and 0.6 mg N/L, respectively, and the concentrations of nitrite were about 0.3 mg N/L, which does not exceed regulatory level of 1.0 mg N/L (WHO).

The influent nitrate and sulfate loading and volumetric denitrification and sulfate reduction were shown in Figures 3 and 4, respectively.

From Run I to Run III, the average nitrate volumetric loading rate increased from 56.5 to 139.5 g N/m^3d, and the

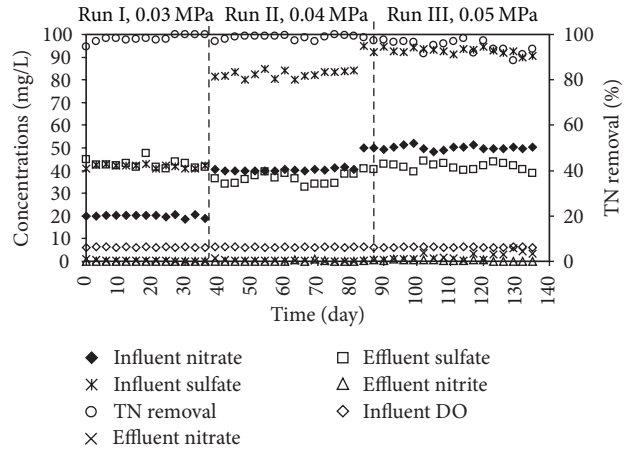

Figure 2: The nitrate, nitrite, sulfate, DO, and TN removal in the continuous experiments.

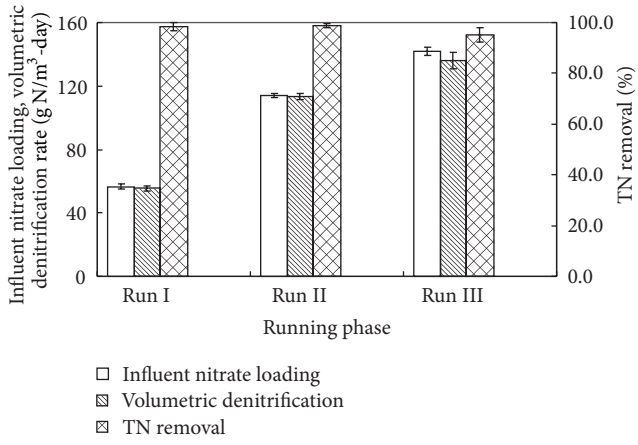

Figure 3: Influent nitrate loading, volumetric denitrification rate, and TN removal in the experiment. Error bars represent the standard deviation between continuous samples during one running phase.

average volumetric denitrification rates were 55.5, 131.1, and 133.8, respectively, which corresponded to average surface denitrification rates of 0.49, 0.98, and 1.18 g N/m^2d, respectively. The average TN removal rate at Run I to Run III reached 98.3%, 98.8%, and 95.0%, respectively, while, at influent of 12.5 mg NO_3^--N/L and hydrogen pressure of 0.42 atm, Lee and Rittmann [17] achieved 1.0 g N/m^2d using the MBfR with 1-micron thick layer of nonporous polyurethane with microporous polyethylene on the inner and outer sides. With the same materials as that of Rittmann, a denitrification rate of 1.4 g N/m^2d was got by Shin et al. [23] using a serial MBfR (nitrification and denitrification) under the condition

Table 3: Electronic-equivalent fluxes for sulfate and nitrate.

Period	Denitrification rate or substrate flux[a]			Electron-equivalent flux (eq/m^2d)				Distribution of electron-equivalent fluxes (%)		
	Nitrate (g/m^2d)	Sulfate (g SO_4^{2-}/m^2d)	O_2 (g/m^2d)	Nitrate[b]	Sulfate[c]	O_2[d]	Sum-up of the fluxes	Nitrate	Sulfate	O_2
Run I	0.49	0.45	0.15	0.18	0.04	0.02	0.23	76.0	15.9	8.1
Run II	0.98	0.75	0.15	0.35	0.06	0.02	0.43	81.5	14.2	4.3
Run III	1.18	0.97	0.15	0.42	0.08	0.02	0.52	81.2	15.2	3.6

[a]Calculated by $J_{substrate}$ = (influent flow rate (Q) × removed substrate (ΔS))/(area of biofilm surface (A_B)), where Q is in m^3/d, ΔS is in g-substrate (NO_3^--N or SO_4^{2-})/m^3, A_B is in m^2, and J is in g-NO_3^--N/m^2d or g-SO_4^{2-}/m^2d.

[b]Calculated by $J_{e^-NO_3^-}$ = (influent flow rate (Q) × removed NO_3^--N (ΔS))/(area of biofilm surface (A_B) × $EW_{Nitrate}$), where Q is in m^3/d, ΔS is in g-NO_3^--N/m^3, A_B is in m^2, $EW_{Nitrate}$ is in 14 g-NO_3^--N/5 e^- equivalent for reduction of nitrate to nitrogen gas, and J is in g-NO_3^--N/m^2d. We assume five electrons per mole for nitrate reduction to nitrogen gas.

[c]Calculated by $J_{e^-SO_4^{2-}}$ = (influent flow rate (Q) × removed SO_4^{2-} (ΔS))/(area of biofilm surface (A_B) × $EW_{Sulfate}$), where Q is in m^3/d, ΔS is in g-SO_4^{2-}/m^3, A_B is in m^2, $EW_{Sulfate}$ is in 96 g-NO_3^--N/8 e^- equivalent for reduction of sulfate to sulfide, and J is in g-SO_4^{2-}/m^2d. We assume 8 electrons per mole for sulfate reduction to sulfide, for seen $SO_4^{2-} + 4H_2 + 1.5H^+ \rightarrow 0.5H_2S + 0.5HS^- + 4H_2O$ (i) [26].

[d]Calculated by $J_{e^-O_2}$ = (influent flow rate (Q) × removed O_2 (ΔS))/(area of biofilm surface (A_B) × EW_{Oxygen}), where Q is in m^3/d, ΔS is in g-O/m^3, A_B is in m^2, EW_{Oxygen} is in 32 g-O_2/4 e^- equivalent for reduction of O_2 to O^{2-}, and J is in g-O_2/m^2d. We assume 4 electrons per mole for reduction O_2 to O^{2-}, for seen $O_2 + 4H^+ \rightarrow 2H_2O$ (ii).

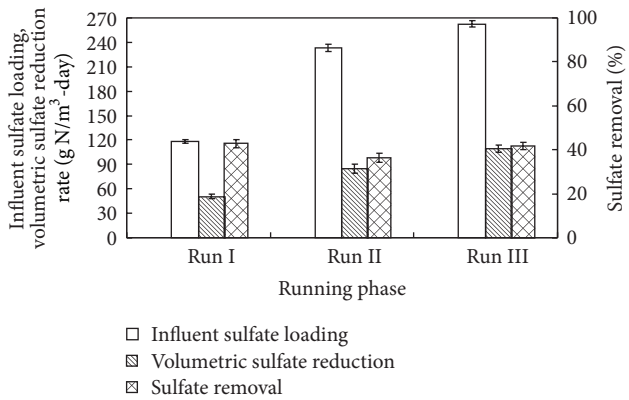

Figure 4: Influent sulfate loading, volumetric sulfate reduction rate, and sulfate removal in the experiment. Error bars represent the standard deviation between continuous samples during one running phase.

of influent nitrate concentration of 51 mg N/L and hydrogen pressure of 4 psi (about 0.3 atm). The influent sulfate loading was varied from 118.5, 233.3, and 262.6 mg SO_4^{2-}/L, with the sulfate reduction loading rates of 50.7, 84.6, and 109.6 mg SO_4^{2-}/L, respectively. And the sulfate removals were 42.8%, 36.2%, and 41.8%, respectively, for the three phases.

3.2. Flux Analysis. Table 3 showed the average values of substrate fluxes and electron-equivalent fluxes for all the electron acceptors, along with the percentage distribution of each flux. With the increasing of influent nitrate concentrations, the oxygen flux reduced. For the distribution of electron-equivalent fluxes, with the influent nitrate concentration increasing, the nitrate fluxes and sulfate fluxes increased, while the O_2 fluxes contained a constant with the effluent DO that was near zero. The results indicated that the autotrophic denitrifiers could utilize DO and nitrate preferentially rather than sulfate. On the other hand, the electron-equivalent fluxes of the nitrate accounted for more than 80% at Run II and Run III, while the electron-equivalent fluxes of sulfate and oxygen account for about 14.2% and 4.3%, respectively, at Run II; the electron-equivalent fluxes of sulfate and oxygen account for about 15.2% and 3.6%, respectively, at Run III. Therefore, with the influent nitrate loading increasing, the oxygen electron-equivalent fluxes decreased, which indicated that the 6.0 mg/L of DO concentration did not affect the nitrate removing from the groundwater [24].

The DO, nitrite, and nitrate in the effluent were very low, while the sulfate in the effluent was about half of its influent concentrations. The results about the sulfate reduction rate were consistent with those reported by Terada et al. [19]; they used a membrane-fibrous composite matrix (a poly membrane tube of dimethylsiloxane and silicone inner and a fibrous support covered the surface of the tube) to immobilize autohydrogenotrophic denitrifying bacteria in the reactor, and they found that, with the hydrogen pressure increased up to 50 kPa, only approximately 50% of sulfate was reduced by SRB. Zhao et al. [25] also reported that the nitrate and oxygen surface loading greater than 0.34 g H_2/m^2·d could suppress the sulfate reduction in MBfR; that is, an appropriate range of nitrate and oxygen surface loading is essential to reduce other oxidized contaminants, such as chlorate and sulfate. The results mean the nitrate and oxygen were easier to get electrons than sulfate when the three electron acceptors were sufficient in autohydrogenotrophic denitrification processes [26].

3.3. Hydrogen Utilization. From Table 3, we can see that hydrogen consumption was mainly attributed to nitrate and sulfate reduction. According to Lee and Rittmann [15], with analyzing the hydrogen utilization of the system, the mass

balances of hydrogen, nitrate, nitrite, and sulfate in the autohydrogenotrophic biofilm were built under the fundamental assumptions. The assumptions are as follows: the substrate utilized by the suspended biomass is ignored and biomass is not included in the mass balances. Since hydrogen utilization for denitrification, sulfate reduction, and oxygen reduction follows the stoichiometry described in (1)–(5) and (i) and (ii) of Table 3, the sum of hydrogen consumption rates during denitrification and sulfate reduction by the biofilm ($R_{H,B}$, mg H_2/cm^3d) can be described by the following and the hydrogen flux ($J_{H,T}$, mg H_2/cm^2d) can be described by the following:

$$R_{H,B}V = \alpha_{H,3}Q\left(S_{3,i} - S_{3,o}\right) + \alpha_{H,2}\alpha_{2,3}Q\left(S_{3,i} - S_{3,o}\right) + \alpha_{H,4}Q\left(S_{4,i} - S_{4,o}\right) + \alpha_{H,5}Q\left(S_{5,i} - S_{5,o}\right) - \alpha_{H,2}QS_{2,o}, \quad (6)$$

$$J_{H,T}A_B = R_{H,B}V + QS_{H,o}, \quad (7)$$

where $R_{H,B}$ is the rate of hydrogen utilization by the biofilm (mg H_2/cm^3d). $\alpha_{H,3}$ is the stoichiometric consumption ratio of hydrogen to nitrate during nitrate reduction (mg H_2/mg N), $\alpha_{H,2}$ is the stoichiometric consumption ratio of hydrogen to nitrite during nitrite reduction to N_2 gas (mg H_2/mg N), and $\alpha_{H,4}$ is the stoichiometric consumption ratio of hydrogen to sulfate during sulfate reduction to sulfide (mg H_2/mg SO_4^{2-}). Based on the stoichiometric reactions of (1) to (5) and (i) and (ii) of Table 3, $\alpha_{H,3}$, $\alpha_{H,2}$, $\alpha_{H,4}$, and $\alpha_{H,5}$ are 0.143, 0.214 mg H_2/mg N, and 0.083 mg H_2/mg SO_4^{2-} and 0.215 mg H_2/mg O_2, respectively. $\alpha_{2,3}$ is the stoichiometric coefficient for the production of nitrite from nitrate to nitrite, which is equal to 1 mg N/mg N. A_B is the biofilm surface area (cm^2), Q is the influent flow rate of the reactor system (l/d), and V is the volume of the reactor (cm^3). $S_{3,i}$ and $S_{3,o}$ are the nitrate concentrations in the influent and the effluent, respectively (mg N/L); $S_{4,i}$ and $S_{4,o}$ are the sulfate concentrations in the influent and the effluent, respectively (mg SO_4^{2-}/L); $S_{5,i}$ and $S_{5,o}$ are the DO concentrations in the influent and the effluent, respectively (mg O_2/L); $S_{H,o}$ is hydrogen concentration in the effluent (mg H_2/L). Then, the rate of hydrogen utilization by the biofilm, the hydrogen concentration in the effluent, and the hydrogen flux in the experiment are demonstrated in Figure 5.

In Run III, the average rate of hydrogen utilization by biofilm was better than that of Run I and Run II, that is, 0.060 mg H_2/cm^3d (0.034 mg H_2/cm^2d) (Figure 5). The results showed that the hydrogen utilization rate increased with the increasing of influent nitrate loading, which indicated this hydrogen pressure (or hydrogen flux) was enough to remove the nitrate from the groundwater, and there still was a potential for a higher influent nitrate loading. These results were consistent with those reported by Lee and Rittmann [15], and Figure 5 also illustrates the effluent hydrogen concentration decreased as the nitrate loading increased and then leveled off at the last running stages, averaged 121 ± 49 μg/L in Run III. This result indicated that the nitrate loading limitation for autohydrogenotrophic denitrification was transited to hydrogen limitation at the stage of effluent hydrogen concentration leveling off, and hydrogen utilization rate was not influenced by sulfate and DO.

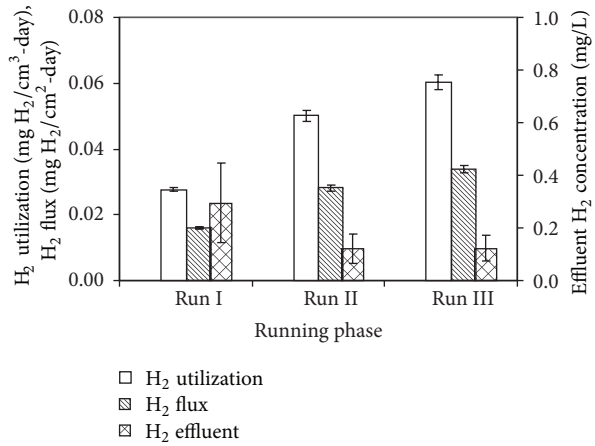

Figure 5: Average rate of hydrogen utilization by the biofilm, average hydrogen concentration in the effluent, and average hydrogen flux at different experimental periods.

Table 4: The H_2 utilization in the MBfR.

	Sum of H_2 utilization (%)	H_2 utilization for NO_3^- (%)	H_2 utilization for SO_4^{2-} (%)	H_2 utilization for O_2 (%)
Run I	96.9 ± 1.6	81.0 ± 1.6	15.9 ± 0.7	12.0 ± 0.4
Run II	99.3 ± 0.3	85.3 ± 0.9	14.0 ± 0.9	6.8 ± 0.3
Run III	99.4 ± 0.2	84.4 ± 0.9	15.0 ± 0.8	6.0 ± 0.4

The percent unutilized hydrogen was calculated as the ratio of H_2 leaving in the effluent divided by the H_2 used for nitrate reduction, nitrite reduction, sulfate reduction, oxygen reduction, and loss to the effluent, as shown in (8). Based on the percent unutilized hydrogen in the experiment, the percent utilized hydrogen could be calculated correspondingly. The results were shown in Table 4.

The hydrogen utilization efficiency in Run I was about 96.9 ± 1.6%, a little bit lower than that of Run II and Run III, which could be explained by the fact that the influent nitrate loading was lower, and the nitrate loading should be the limiting factor for denitrification at Run I:

$$\%H_2 \text{ unutilized} = 100\% \times \left(S_{H,o}\right) \times \left(0.143\left(S_{3,i} - S_{3,o}\right) + 0.214\left(S_{3,i} - S_{3,o} - S_{2,o}\right) + 0.083\left(S_{4,i} - S_{4,o}\right) + 0.125\left(S_{5,i} - S_{5,o}\right) + S_{H,o}\right)^{-1}. \quad (8)$$

3.4. Membrane Scaling Potential. At the denitrification process, the pH will increase because of alkalinity production (5), which can result in precipitation of $CaCO_3$ on the fibers [15, 27], blocking the pores of the membranes and limiting

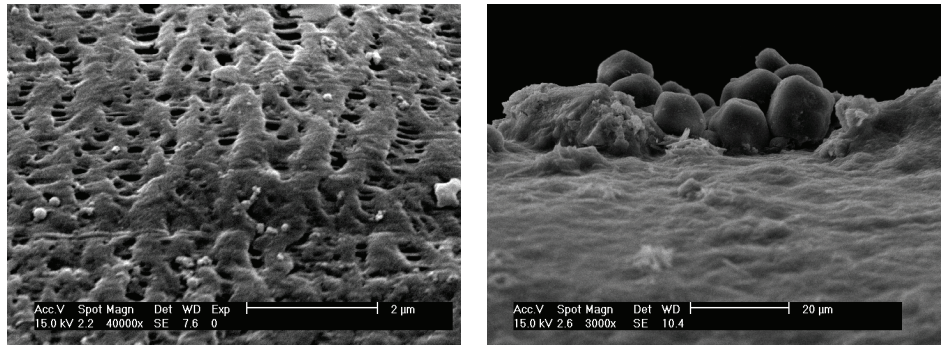

(a) (b)

Figure 6: The scanning electron micrograph of control hollow fiber membrane surface (a) and polluted membrane from MBfR (b).

H_2 transfer across the micropores of the membrane. The membrane scaling potential by $CaCO_3$ was analyzed by the Langelier Saturation Index (LSI), which indicated whether or not the water was supersaturated:

$$\mathrm{LSI} = \mathrm{pH_a} - \mathrm{pH_s}, \tag{9}$$

where $\mathrm{pH_a}$ is the measured pH and $\mathrm{pH_s}$ is the theoretical pH of the water if it were in equilibrium with $CaCO_3$ and calculated as

$$\mathrm{pH_s} = \mathrm{pK_{a,HCO_3^-}} - \mathrm{pK_{SO}} + \mathrm{p}\left[\mathrm{Ca^{2+}}\right] + \mathrm{p}\left[\mathrm{HCO_3^-}\right] - \log r_{\mathrm{Ca^{2+}}} - \log r_{\mathrm{HCO_3^-}}, \tag{10}$$

$$\lg r_i = -Az_i^2 I^{1/2}, \tag{11}$$

$$I = 2.5 \times 10^{-5} \times \mathrm{TDS} \tag{12}$$

in which $\mathrm{pK_{a,HCO_3^-}}$ is the HCO_3^- acid dissociation constant ($10^{-10.33}$ at 25°C), K_{SO} is the solubility production for $CaCO_3$ ($10^{-8.34}$ at 25°C), and $[Ca^{2+}]$ is measured alkalinity (M). $r_{Ca^{2+}}$ and $r_{HCO_3^-}$ are the activity coefficients for Ca^{2+} and HCO_3^-, respectively. I is the ionic strength in mg/L.

Based on the average influent water quality of pH 7.6, TDS 300 mg/L, alkalinity 510 mg/L (as $CaCO_3$), and hardness 200 mg/L (as $CaCO_3$), the LSI was 0.4 in the effluent calculated by the above equations, which indicated that the membrane was at the risk of surface scaling. The LSI values were a little higher than that (LSI, 0.11 in the effluent) of the report by Ziv-El and Rittmann [24] who used MBfR to reduce the perchlorate from the groundwater, based on the groundwater of pH 7.5, DO 7.9 mg/L, alkalinity 230 mg $CaCO_3$/L, TDS 490 mg/L, and hardness 410 mg $CaCO_3$/L. For the MBfR running successfully, CO_2 was added to the reactor to lower the pH to prevent precipitation, even though the SEM of the biofilm at Run III showed that there was some membrane fouling (Figure 6). From Figure 6, the membrane micropores of the control fiber were homogenous (Figure 6(a)), while the precipitation particles at membrane fiber got at 130d were obvious.

4. Conclusion

From the 135 days of operations, the results showed that the continuous stirred PVC MBfR could remove nitrate effectively from the groundwater on site. The average denitrification rates of 133.8 g NO_3^--N/m^2d (1.18 g NO_3^--N/m^2d) were achieved at influent nitrate concentration 50 mg N/L and hydrogen pressure 0.05 MPa. The fluxes analysis showed that the electron-equivalent fluxes of sulfate and oxygen account for about 15.2% and 3.6%, respectively, at the conditions of actual influent, which indicated that nitrate reduction could consume more electrons than that of sulfate reduction and dissolved oxygen reduction. The nitrate reduction was not significantly influenced by sulfate reduction and the dissolved oxygen reduction. Based on the actual quality on site, the membrane could be at the risk of surface scaling; therefore, the reactor should be considered as the scaling control in the operation application.

Conflict of Interests

The authors declare that there is no conflict of interests regarding the publication of this paper.

Acknowledgments

This research was supported fancily by the Natural Science Foundation of Shandong Province (no. BS2013HZ028) and the State Key Laboratory of Pollution Control and Resource Reuse Foundation (no. PCRRF12017). The authors thank the Department of Environmental Protection of Shandong Province (no. SDHBYF-2012-14) and the National Natural Science Foundation of China (no. 51408588) for their kind support.

References

[1] D. C. Bouchard, M. K. Williams, and R. Y. Surampalli, "Nitrate contamination of groundwater: sources and potential health effects," *The American Water Works Association*, vol. 84, no. 9, pp. 85–90, 1992.

[2] Q. Wang, C. Feng, Y. Zhao, and C. Hao, "Denitrification of nitrate contaminated groundwater with a fiber-based biofilm reactor," *Bioresource Technology*, vol. 100, no. 7, pp. 2223–2227, 2009.

[3] D. J. Wan, H. J. Liu, X. Zhao, J. H. Qu, S. H. Xiao, and Y. Hou, "Role of the Mg/Al atomic ratio in hydrotalcite-supported Pd/Sn catalysts for nitrate adsorption and hydrogenation reduction," *Journal of Colloid and Interface Science*, vol. 332, no. 1, pp. 151–157, 2009.

[4] B.-U. Bae, Y.-H. Jung, W.-W. Han, and H.-S. Shin, "Improved brine recycling during nitrate removal using ion exchange," *Water Research*, vol. 36, no. 13, pp. 3330–3340, 2002.

[5] J. J. Schoeman and A. Steyn, "Nitrate removal with reverse osmosis in a rural area in South Africa," *Desalination*, vol. 155, no. 1, pp. 15–26, 2003.

[6] A. El Midaoui, F. Elhannouni, M. Taky et al., "Optimization of nitrate removal operation from ground water by electrodialysis," *Separation and Purification Technology*, vol. 29, no. 3, pp. 235–244, 2002.

[7] J. W. Peel, K. J. Reddy, B. P. Sullivan, and J. M. Bowen, "Electrocatalytic reduction of nitrate in water," *Water Research*, vol. 37, no. 10, pp. 2512–2519, 2003.

[8] M. Shrimali and K. P. Singh, "New methods of nitrate removal from water," *Environmental Pollution*, vol. 112, no. 3, pp. 351–359, 2001.

[9] R. L. Smith, M. L. Ceazan, and M. H. Brooks, "Autotrophic, hydrogen-oxidizing, denitrifying bacteria in groundwater, potential agents for bioremediation of nitrate contamination," *Applied and Environmental Microbiology*, vol. 60, no. 6, pp. 1949–1955, 1994.

[10] M. A. Gómez, E. Hontoria, and J. González-López, "Effect of dissolved oxygen concentration on nitrate removal from groundwater using a denitrifying submerged filter," *Journal of Hazardous Materials*, vol. 90, no. 3, pp. 267–278, 2002.

[11] D. Dries, J. Liessens, W. Verstraete, P. Stevens, P. De Vos, and J. De Ley, "Nitrate removal from drinking water by means of hydrogenotrophic denitrifiers in a polyurethane carrier reactor," *Water Supply*, vol. 6, no. 3, pp. 181–192, 1988.

[12] A. Kapoor and T. Viraraghavan, "Nitrate removal from drinking water—review," *Journal of Environmental Engineering*, vol. 123, no. 4, pp. 371–380, 1997.

[13] M. Kurt, I. J. Dunn, and J. R. Bourne, "Biological denitrification of drinking water using autotrophic organisms with H_2 in a fluidized-bed biofilm reactor," *Biotechnology and Bioengineering*, vol. 29, no. 4, pp. 493–501, 1987.

[14] H. Hasar, "Simultaneous removal of organic matter and nitrogen compounds by combining a membrane bioreactor and a membrane biofilm reactor," *Bioresource Technology*, vol. 100, no. 10, pp. 2699–2705, 2009.

[15] K.-C. Lee and B. E. Rittmann, "Applying a novel autohydrogenotrophic hollow-fiber membrane biofilm reactor for denitrification of drinking water," *Water Research*, vol. 36, no. 8, pp. 2040–2052, 2002.

[16] K. S. Haugen, M. J. Semmens, and P. J. Novak, "A novel in situ technology for the treatment of nitrate contaminated groundwater," *Water Research*, vol. 36, no. 14, pp. 3497–3506, 2002.

[17] K.-C. Lee and B. E. Rittmann, "A novel hollow-fibre membrane biofilm reactor for autohydrogenotrophic denitrification of drinking water," *Water Science and Technology*, vol. 41, no. 4-5, pp. 219–226, 2000.

[18] S. J. Ergas and A. F. Reuss, "Hydrogenotrophic denitrification of drinking water using a hollow fibre membrane bioreactor," *Journal of Water Supply: Research and Technology*, vol. 50, no. 3, pp. 161–171, 2001.

[19] A. Terada, S. Kaku, S. Matsumoto, and S. Tsuneda, "Rapid autohydrogenotrophic denitrification by a membrane biofilm reactor equipped with a fibrous support around a gas-permeable membrane," *Biochemical Engineering Journal*, vol. 31, no. 1, pp. 84–91, 2006.

[20] NEPA, *Water and Wastewater Monitoring Methods*, Chinese Environmental Science Publishing House, Beijing, China, 2002.

[21] Y. Zhang, F. Zhong, S. Xia, X. Wang, and J. Li, "Autohydrogenotrophic denitrification of drinking water using a polyvinyl chloride hollow fiber membrane biofilm reactor," *Journal of Hazardous Materials*, vol. 170, no. 1, pp. 203–209, 2009.

[22] S. Xia, Y. Zhang, and F. Zhong, "A continuous stirred hydrogen-based polyvinyl chloride membrane biofilm reactor for the treatment of nitrate contaminated drinking water," *Bioresource Technology*, vol. 100, no. 24, pp. 6223–6228, 2009.

[23] J. H. Shin, B. I. Sang, Y. C. Chung, and Y. K. Choung, "A novel CSTR-type of hollow fiber membrane biofilm reactor for consecutive nitrification and denitrification," *Desalination*, vol. 221, no. 1–3, pp. 526–533, 2008.

[24] M. C. Ziv-El and B. E. Rittmann, "Systematic evaluation of nitrate and perchlorate bioreduction kinetics in groundwater using a hydrogen-based membrane biofilm reactor," *Water Research*, vol. 43, no. 1, pp. 173–181, 2009.

[25] H.-P. Zhao, A. Ontiveros-Valencia, Y. Tang et al., "Using a two-stage hydrogen-based membrane biofilm reactor (MBfR) to achieve complete perchlorate reduction in the presence of nitrate and sulfate," *Environmental Science and Technology*, vol. 47, no. 3, pp. 1565–1572, 2013.

[26] J. Chung, R. Nerenberg, and B. E. Rittmann, "Bioreduction of selenate using a hydrogen-based membrane biofilm reactor," *Environmental Science and Technology*, vol. 40, no. 5, pp. 1664–1671, 2006.

[27] K. C. Lee and B. E. Rittmann, "Effects of pH and precipitation on autohydrogenotrophic denitrification using the hollow-fiber membrane-biofilm reactor," *Water Research*, vol. 37, no. 7, pp. 1551–1556, 2003.